Interaction and motion of solitons in passively-mode-locked fiber lasers

Xueming Liu

Phys. Rev. A **84**, 053828 — Published 14 November 2011

DOI: 10.1103/PhysRevA.84.053828

Interaction and motion of solitons in passively mode-locked fiber lasers

Xueming Liu

State Key Laboratory of Transient Optics and Photonics, Xi'an Institute of Optics and Precision Mechanics, Chinese Academy of Sciences, Xi'an 710119, China

liuxueming72@yahoo.com

Interaction and motion of multiple solitons in passively mode-locked (PML) fiber lasers are investigated numerically. Three types of relative motions of two solitons are found in PML fiber lasers. The numerical results show that the relative motion of solitons attributes to the phase shift, which corresponds to the instantaneous frequency of soliton to be nonzero. Different from the classical dynamics of billiard balls, the interaction of solitons is similar to Feynman diagram that is a pictoral way to represent the interaction of particles. After solitons interact with one another, their shapes do not change, but their phases shift and relative motions change. The theoretical results demonstrate that the separation of neighboring solitons in laser cavity is about several hundreds of picosecond to several nanosecond. The theoretical predictions are in good agreement with the experimental results.

PACS number(s): 42.65.Tg, 42.81.Dp, 42.55.Wd, 42.65.Re

I. INTRODUCTION

Passively mode-locked (PML) fiber lasers can provide the simple and economic ultrashort-pulse sources [1]-[4]. They constitute an ideal platform for exploring new areas of nonlinear dynamics [5]. Multiple soliton operation in PML fiber lasers, which has been investigated extensively [2]-[6], is the typical result of the conjunction of a relatively strong pumping power. Solitons observed in fiber lasers exhibit special features such as the soliton bounding, the soliton bunching, and the quasi-harmonic and harmonic mode locking. Bound solitary pulses, so-called soliton molecules

[2][7], have attracted a great deal of interest due to their important potential applications. Bound states of solitons can be predicted in the coupled nonlinear Schrödinger equations (NLSEs) [7][8] and the quintic complex Ginzburg-Landau equation [9]. Investigations on the interaction between the bound solitons show that the bound pulses always behave as a unit. Usually, the peak-to-peak (P2P) separation of bound solitons is less than several pulse-duration [2][7]-[9].

Different from the bound states of solitons, the P2P separation of soliton bunching can be over tens of times larger than the pulse width. Pulse bunching is a special behavior that corresponds to the ability of several identical soliton pulses to cluster themselves in a packet.

The formation and evolution of multiple solitons are studied numerically and experimentally by many authors [3][8][10][11]. Various features such as the pump power hysteresis, multi-soliton generation, and various modes of multi-soliton operation were observed experimentally and investigated theoretically. Tang *et al.* proved that the soliton shaping of the dispersive waves or the continuous-wave (cw) components plays a key role on the generation of additional solitons [8]. In our previous reports, it is proved that the mechanism of pulse splitting determines the dual- and multi-soliton generation in the net-anomalous-dispersion fiber lasers [12], whereas two pulses are gradually formed at the cost of dropping off a pulse in the net-normal-dispersion fiber lasers [7]. Theoretical and experimental results show that the PML fiber lasers alternately evolve on the stable and unstable mode-locking states as a function of the pump strength [3].

An important characteristic of the multi-soliton operation of the laser is that solitons always have erratic motions. A typically experimental result is demonstrated in Fig. 1. The experimental setup and parameters are shown in our previous report [12]. The experimental observations show that solitons in the cavity have erratic relative motions. It is import to have a clear understanding of the physical mechanism responsible for the relative motion of solitons in the PML fiber lasers.

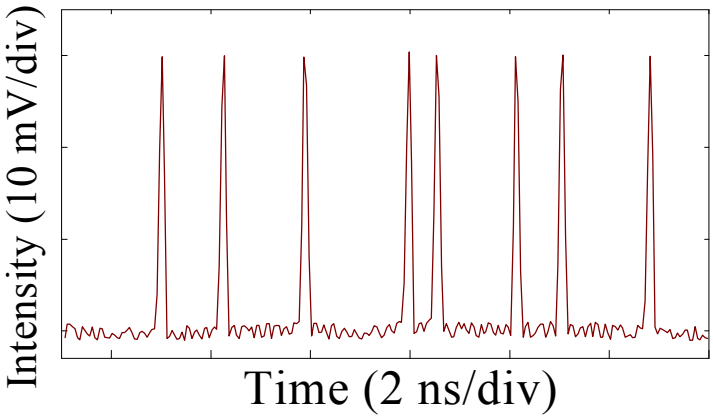

FIG. 1. (Color online) A typical example for the experimentally measured oscilloscope trace of the multi-soliton operation of the PML fiber laser. The separation of neighboring solitons is about several hundreds of ps to several ns. The output average power is about 1.2 mW.

Although some numerical and experimental investigations for multi-soliton operation were reported [3][8][13][14], the investigations for physical mechanism describing the multi-soliton behavior are scarce. In our previous report [12], although the multi-soliton formation and evolution were studied numerically and experimentally in PML fiber lasers, the physical mechanism is ignored. How may types of the relative motions of intracavity solitons are there in PML fiber lasers? What is the inherent mechanism that the intracavity solitons have erratic relative motions and stabilize themselves at more or less random relative positions? The current work answers these questions. Three types of the relative motions of solitons are found in this report. The numerical simulations show that solitons have exactly the same pulse properties when they are the steady state. It is found that the phase shift determines what and how solitons move. Soliton collision in PML fiber lasers is similar to Feynman diagram, rather than the billiard ball collision.

II. MODELING

In current work, the nonlinear polarization evolution technique contributes to the passive mode locking of the laser. The two coupled NLSEs that involve a vector electric field can model the lightwave propagation in the weakly birefringent fibers accurately. The coupled equations are expressed by [3][15][16]

$$\frac{\partial u}{\partial z} = -\frac{\alpha}{2}u - \delta\frac{\partial u}{\partial T} - i\frac{\beta_2}{2}\frac{\partial^2 u}{\partial T^2} + i\gamma\left(|u|^2 + \frac{2}{3}|v|^2\right)u + \frac{g}{2}u + \frac{g}{2\Omega_g^2}\frac{\partial^2 u}{\partial T^2},$$

$$\frac{\partial v}{\partial z} = -\frac{\alpha}{2}v + \delta\frac{\partial v}{\partial T} - i\frac{\beta_2}{2}\frac{\partial^2 v}{\partial T^2} + i\gamma\left(|v|^2 + \frac{2}{3}|u|^2\right)v + \frac{g}{2}v + \frac{g}{2\Omega_g^2}\frac{\partial^2 v}{\partial T^2}, \quad (1)$$

where u and v denote the envelopes of the optical pulses along the two orthogonal polarization axes of the fiber. They are complex functions that depend on T and z. T and z represent the time and the propagation distance, respectively. α, δ, β_2, γ, and Ω_g are the loss coefficient of fiber, the group velocity difference between the two polarization modes, the fiber dispersion, the cubic refractive nonlinearity of the medium, and the bandwidth of the laser gain, respectively. g is the net gain, which describes the gain function of doped fiber. It is expressed by $g = g_0 \exp\left(-E_p / E_s\right)$ [17], where g_0, E_s, and E_p are the small-signal gain, the gain saturation energy (it is pump-power dependent [3]), and the pulse energy, respectively. When the soliton propagates through the laser cavity, the intensity transmission T_i is expressed as

$$T_i = \sin^2(\theta)\sin^2(\varphi) + \cos^2(\theta)\cos^2(\varphi) + 0.5\sin(2\theta)\sin(2\varphi)\cos(\phi_1 + \phi_2), \quad (2)$$

where ϕ_1 is the phase delay caused by the polarization controllers and ϕ_2 is the phase delay resulting from the fiber, including both the linear phase delay and the nonlinear phase delay. The polarizer and analyzer have an orientation of angles θ and φ with respect to the fast axis of the fiber, respectively [3]. The diagram for θ and φ is illustrated in Refs. [3][15] in detail.

The following parameters are employed for our simulations for possibly matching the experimental conditions: α=0.2 dB/km, g_0=2 m^{-1}, θ=π/3.5, φ=π/10, ϕ_1=0.9+π/2, γ=4.5 $W^{-1}km^{-1}$ for EDF and 1.3 $W^{-1}km^{-1}$ for SMF, Ω_g=30 nm, and β_2=53.5×10^{-3} ps^2/m for EDF and −21.7×10^{-3} ps^2/m for SMF. The length of EDF and SMF is 11 and 702 m, respectively. The above parameters are from the data sheets of fiber products. Obviously, the net dispersion of laser cavity is anomalous so that the laser can deliver the conventional solitons. The schematic diagram of experimental setup is

shown in Ref. [12].

III. SIMULATION RESULTS

A. Intracavity two-soliton and relative motion

To find the characteristics and behaviors of solitons in the proposed laser, the simulation starts from a noise signal and converges into a stable solution at different E_s. Since the saturation energy E_s is proportional to the pumping strength, the increase of E_s in simulations corresponds to increasing the pump power in the experiments [15]. Numerical results show that the pulse number over a cavity round-trip time is generated one by one with the increase of the pumping strength E_s. When E_s is lower than about 15 pJ, no soliton solution exists in the proposed laser. When E_s is from about 15 to 50 pJ, only a soliton exists in the laser cavity. However, there are two solitons simultaneously in the laser cavity while E_s is from about 50 to 90 pJ.

Figure 2 shows the formation and evolution of two solitons from a noise signal at E_s=70 pJ. In simulations, a noise wave is assumed as an initial value. A soliton is formed first and successively it is split into two solitons. The detailed process is shown in Fig. 2(a). Figure 2(b), which is the planform of Fig. 2(a), shows the soliton trajectory in round-trip number N and time space. We can see from Figs. 2(a) and 2(d) that there is chaos process when a soliton is split into two solitons. From Figs. 2(a) and 2(b), one can see that the P2P separation of two solitons increases in the beginning of the round trips and then it gradually approaches a fixed value of about 1.9 ns. Numerical results show that two solitons have exactly the same physics properties (e.g., the same pulse duration and peak power) throughout the evolution of solitons. It is found from Fig. 2(d) that the peak power and pulse duration are oscillating at N<120 and successively they approach about 20.9 W and 3.4 ps, respectively. In the steady state, the P2P separation of solitons is about 560 times as large as the pulse duration.

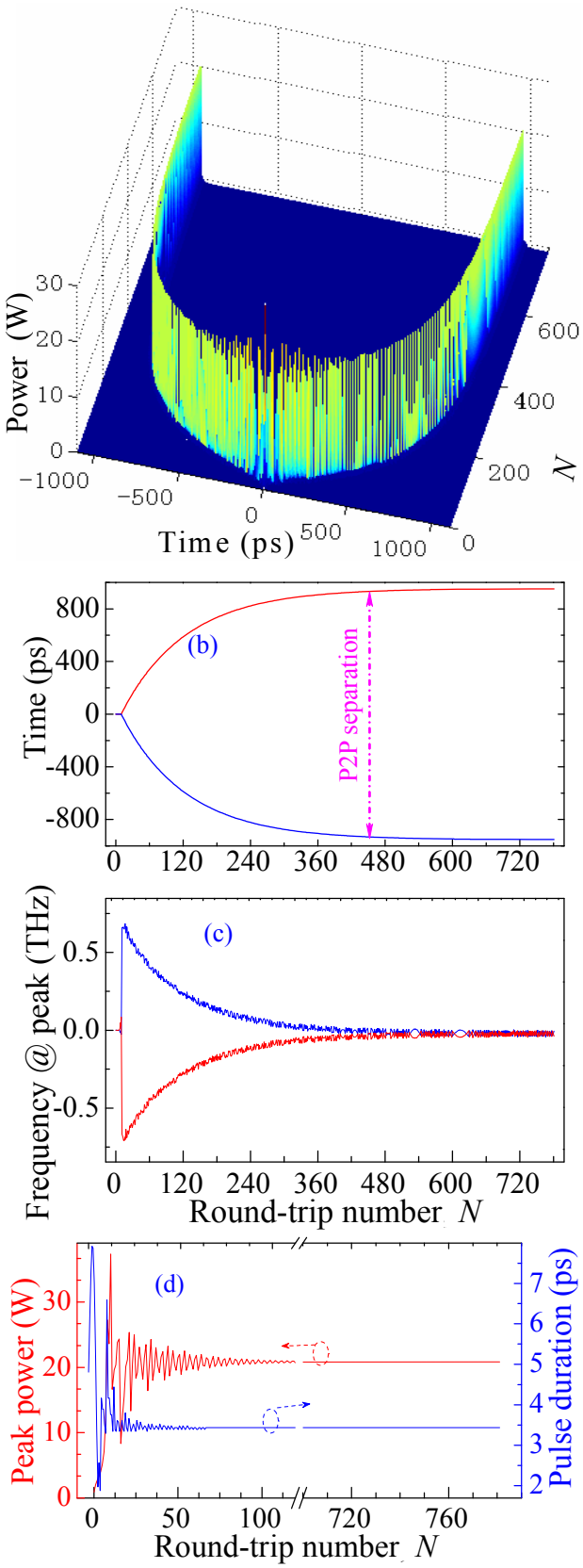

FIG. 2. (Color online) (a) Formation and evolution of solitons from a noise wave. (b) Soliton trajectory in round-trip number N and time space. (c) Instantaneous frequency at pulse peak, F_P, versus N. (d) Peak power and pulse duration versus N. (b) is the planform of (a). E_s=70 pJ.

Figures 2(c) shows the relationship between the instantaneous frequency of soliton at pulse peak, F_P, and round-trip number N. We can observe that, for N<11, there is only a soliton (Fig. 2(b)) and F_P is equal to zero. Successively, a soliton is split into two solitons. When N is from about 13 to 400, two solitons separate from each other gradually (Figs. 2(a) and 2(b)) whereas F_P inchmeal approaches zero (Fig. 2(c)). For N>600, two solitons reach the steady state with the fixed separation of about 1.9 ns and F_P approximately is equal to zero.

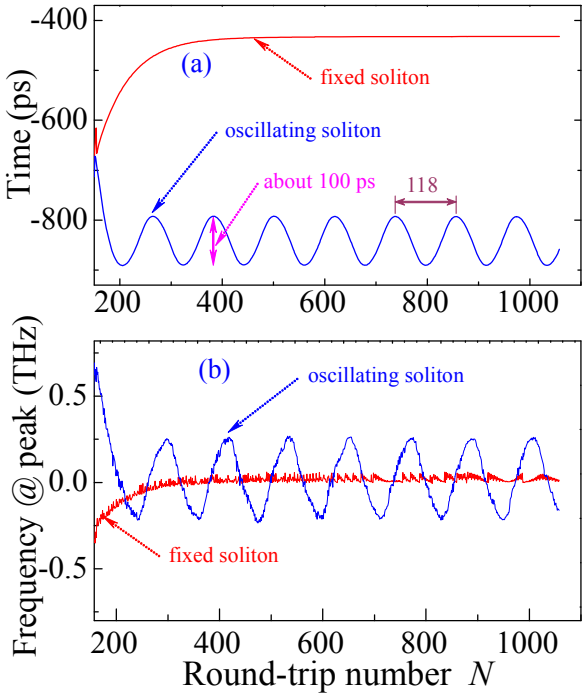

FIG. 3. (Color online) Evolution of two solitons at E_s=81 pJ. (a) Soliton trajectory in round-trip number N and time space. (b) Instantaneous frequency at pulse peak, F_P, versus N.

When E_s is from about 75 to 82 pJ, the relative motion of two solitons is different from Fig. 2 where each soliton approaches a certain position. An example for the evolution of two solitons at E_s=81 pJ is shown in Fig. 3. One can see from Fig. 3(a) that one of solitons evolves to a fixed position whereas the other soliton oscillates with a amplitude of about 100 ps and a period of 118 of round trips. The P2P separation of two solitons periodically oscillates from about 360 to 460 ps for

N>400. It is found that F_P of the oscillating soliton also periodically oscillates along N (Fig. 3(b)), while $F_P \approx 0$ for the fixed soliton.

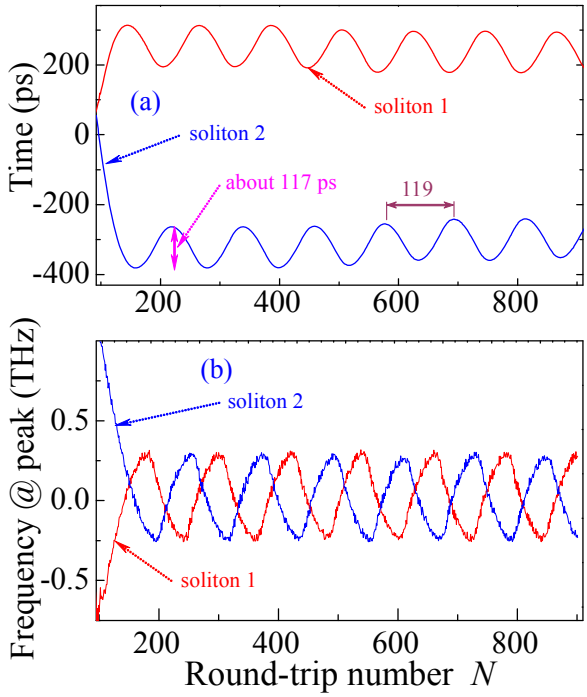

FIG. 4. (Color online) Evolution of two solitons at E_s=85 pJ. (a) Soliton trajectory in round-trip number N and time space. (b) Instantaneous frequency at pulse peak, F_P, versus N.

When E_s is from about 82 to 90 pJ, both F_P and two solitons oscillate along N. Figure 4 demonstrates the evolution of two solitons at E_s=85 pJ. Figure 4(a) exhibits that two solitons oscillate with the amplitude of about 117 ps and the period of 119 of round trips. Two solitons attract and repel each other periodically along N. The P2P separation of solitons periodically oscillates from about 415 to 690 ps for N >150 (Fig. 4(a)).

Obviously, there are three types of relative motions for two solitons in the laser cavity. They evolve with the fixed trajectory (Fig. 2) and the oscillating trajectory for both of two solitons (Fig. 4), as well as the fixed trajectory for a soliton and the oscillating trajectory for another soliton (Fig. 3). The instantaneous frequency at pulse peak, F_P, governs the relative motion of solitons. Solitons evolve to the steady state when F_P approaches zero, whereas they oscillate in the cavity for $F_P \neq 0$.

For an example as shown in Fig. 2, two solitons have the same pulse properties (e.g., the same pulse duration, pulse energy, and phase) with a fixed separation. In this case, the unit of two solitons is very similar to the bound-state solitons except that they have different P2P separations. This type of solitons can be regarded as static soliton pairs. When the relative motion of one or two solitons is oscillating (e.g., Figs. 3 and 4), this kind of solitons can be regarded as dynamic soliton pairs. The theoretical results explain why the intracavity multi-solitons can have erratic relative motions in the experimental observations.

B. Intracavity multi-soliton and collision

When E_s is from about 90 to 125 pJ, three solitons with the same physical properties coexist in the cavity. An example for E_s=96.2 pJ is shown in Fig. 5. One can see that, for N >900, F_P per soliton approximately is equal to zero (Fig. 5(c)) and each soliton evolves to the steady state (Fig. 5(a)). The three solitons have the same pulse profile, pulse duration, and peak power. From Figs. 5(a) and 5(b), we can find a strange phenomenon when N is from about 475 to 500. At this stage, two solitons repel each other and never be merged. The inset of Fig. 5(b) shows that the minimum separation of neighboring solitons is about 35 ps.

According to soliton theory, when solitons interact with other solitons, their shapes do not change, but their phase shifts. Actually, the phenomenon of "phase shift" is a standard feature of soliton interactions. The change of phase leads to the variation of F_P. Note that the instantaneous frequency is the first derivative of phase [18]. Obviously, the numerical simulations here are in excellent agreement with the results in the traditional soliton theory. The theoretical prediction in this paper is very similar to KdV soliton in Ref. [19]. Moreover, Fig. 5(c) shows that F_P at the soliton collision (N≈475 to 500) has the strong fluctuation and the strong phase shift occurs.

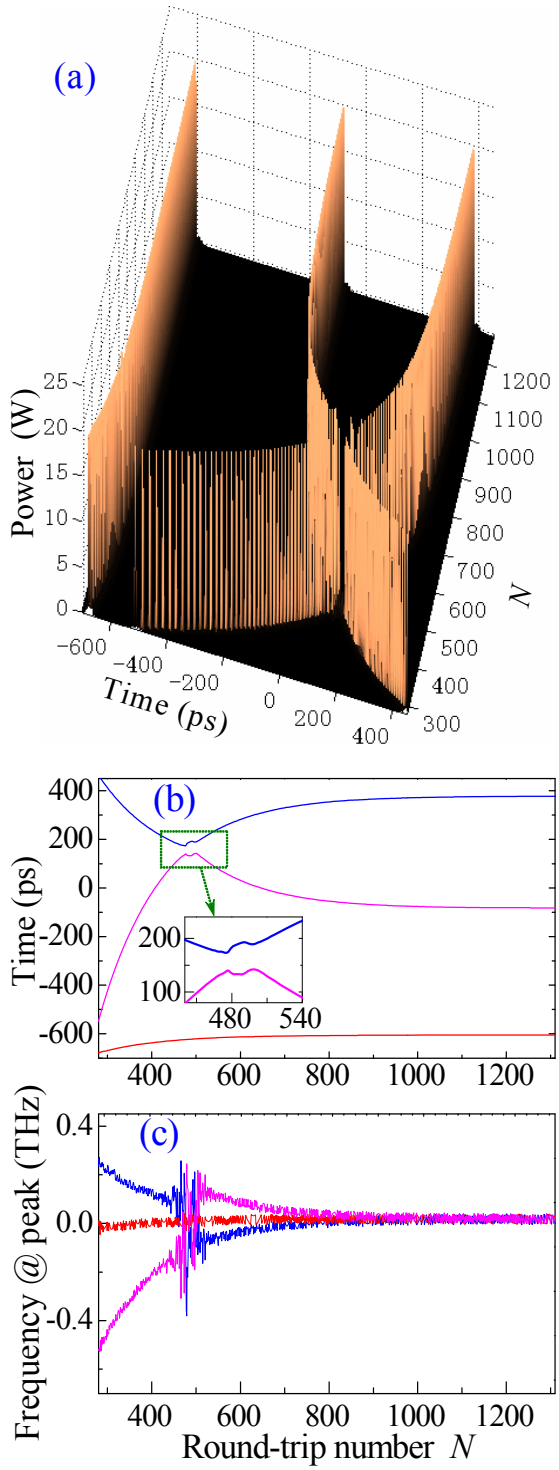

FIG. 5. (Color online) (a) Interaction and evolution of three solitons at E_s=96.2 pJ. (b) Soliton trajectory in round-trip number N and time space. (c) Instantaneous frequency at pulse peak, F_P, versus N. In (b), inset is the local view of the soliton collision. In (c), F_P at N≈475 to 500 has the strong fluctuation and the strong phase shift is incurred.

When E_s is from about 125 to 155, 155 to 185, and 185 to 205 pJ, numerical results shows that four, five, and six solitons coexist in the laser cavity, respectively. Figures 6(a), 6(b), and 6(c) demonstrate three examples at E_s=130, 165, and 200 pJ, respectively. In the simulation, the phase shifts are imposed on some solitons initially. The simulation results exhibit that the solitons imposed by the initial phase shift have the relative motion in the beginning of round trips. After enough round trips, all solitons approach the steady state and F_P of each soliton is near zero. In simulating Fig. 6(c), only a soliton is initially imposed on the phase shift, but the soliton collisions occur four times. Figures 5 and 6 illustrate that the separation of neighboring solitons is nonuniform and the numerical predictions well agree to the experimental observations as shown in Fig. 1. From Figs. 2-6, one can see that the P2P separation of neighboring solitons is about several hundreds of ps to several ns. The experimental results (e.g., Fig. 1) confirm the theoretical predictions.

We can see from Figs. 5 and 6 that, as two solitons get close, they never pass through each other and the transfers of energy and information of solitons are transited by a virtual soliton. Obviously, Figs. 5 and 6 show that the soliton collision in PML fiber lasers is not similar to the billiard ball collision. Rather than the classical dynamics of billiard balls, the interaction of solitons can similarly be interpreted by the Feynman diagram, in which the interaction of two electrons exchange a (virtual) photon and then repel one other [20]. In fact, the particle-like behavior of solitons is discovered in the KdV two-soliton collision, where a virtual "transfer" soliton steal energy from the faster one in the rear and pass it to the soliton in front [19][21]. As a result, solitons are waves that act like particles and even the particle-like behavior of solitons can help us to better understand real particles.

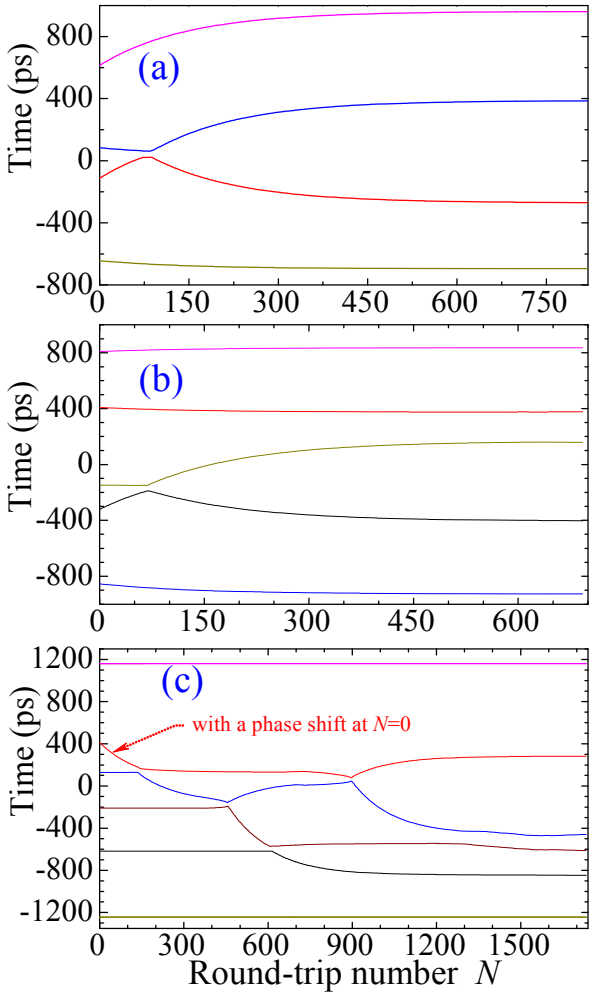

FIG. 6. (Color online) Soliton trajectory in round-trip number N and time space at (a) E_s=130 pJ, (b) E_s=165 pJ, and (c) E_s=200 pJ. Four, five, and six solitons coexist in the laser cavity for (a), (b), and (c), respectively. Although some neighboring solitons get close and collide, they nerve pass through each other. In (c), only a soliton is initially imposed on a phase shift, but the soliton collisions occur four times.

IV. MECHANISM OF MOTION OF SOLITONS

When the separation of solitons is over tens of times larger than the pulse duration, the interaction between solitons is very weak. What is the key role that governs the motion of solitons? From Figs. 2-6, the relative motion of soliton originates from the phase shift.

Our laser is mode-locked by using the nonlinear phase rotation (NPR) technique. The laser

cavity can be simplified to a setup as shown in Fig. 7 [3][8]. The intensity transmission T_i from input to output, as shown in Fig. 7, can be achieved by numerical solving Eqs. (1) and (2). When no phase shift is imposed on solitons (corresponding to F_P=0), the intensity transmission T_i is symmetrical with respect to the relative time (Fig. 8(a)). As a result, no relative motion occurs except that the soliton intensity is attenuated (Fig. 8(b)). However, when the phase shift is imposed on soliton (corresponding to $F_P \neq 0$), T_i is asymmetrical with respect to the relative time (dashed curve in Fig. 8(a)) and then soliton has the relative motion (dashed curve in Fig. 8(b)).

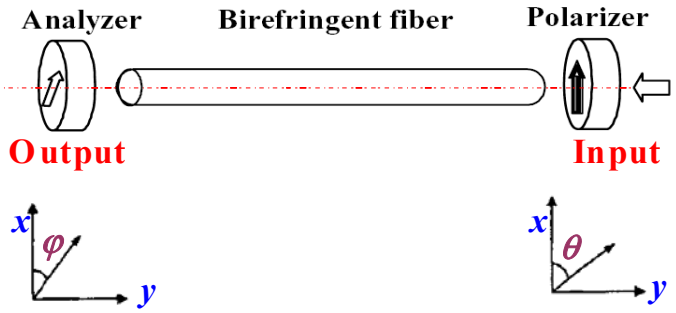

FIG. 7. (Color online) An equivalent setup to NPR element for determining the cavity transmission.

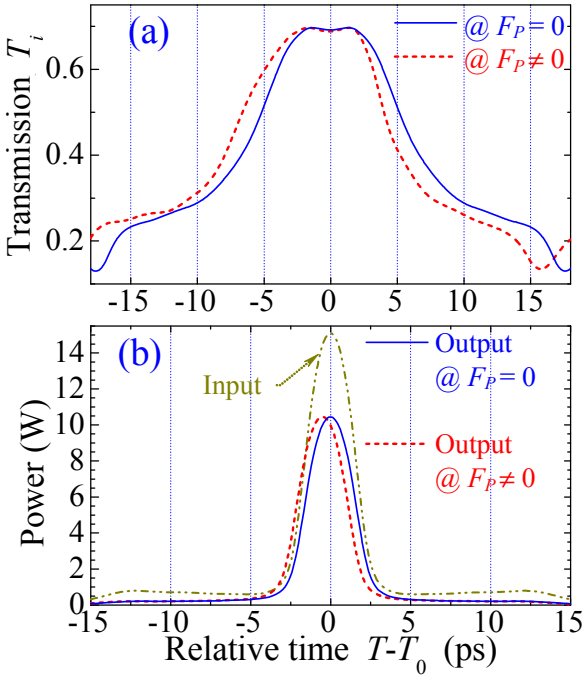

FIG. 8. (Color online) (a) Intensity transmission at F_P=0 and $F_P \neq 0$. (b) Power spectra of solitons before and after NPR element. The solid curve in (a) is symmetric with respect to the relative time, but the dashed curve is asymmetric.

Figure 9 shows the soliton trajectory in intracavity position and time space. In simulations, the phase shift is imposed on soliton-1, but no phase shift on soliton-2. It is easily found from Fig. 9 that there is no relative motion for a soliton without the phase shift, whereas another soliton with the phase shift has the relative motion along the intracavity position. In our previous report, the chirped solitons are narrowed in the beginning of propagation distance and successively they are broadened due to the dispersive effect (Figs. 8 and 9 in Ref. [12]). But, no relative motion occurs for them, similar to the soliton-2 in Fig. 9. Besides the dispersion-induced narrowing and broadening of pulses, the relative motion occurs for the solitons imposed by the phase shift (Soliton-1 in Fig. 9 shows an example). Therefore, the dispersion-induced phase shift plays a key role on the relative motion of soliton in the laser cavity.

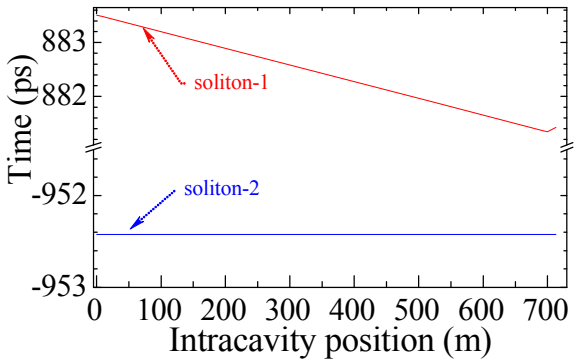

FIG. 9. (Color online) Soliton trajectory in intracavity position and time space. The phase shift is imposed on soliton-1, but no phase shift on soliton-2. There is and is not the relative motion for soliton-1 and soliton-2 along the intracavity position, respectively.

In practice, many parameters of lasers are fluctuant, such as pump power, environmental temperature, refractive index of fiber, and polarization state. These fluctuations will perturb the laser system and may contribute on the phase shift of solitons. Additionally, the soliton collision can induce the strong phase shift, as shown in Fig. 5(c). Figure 6(c) shows that the soliton collision induces the relative motions of multiple solitons along *N*. Therefore, intracavity solitons are easily

imposed by the phase shift in a practical environment so that they often have erratic relative motions and stabilize themselves at more or less random relative positions. The theoretical results are consistent with the experimental observations.

V. CONCLUSIONS

In this paper, we have numerically investigated the evolution and interaction of two and multiple solitons and their relative motions in PML fiber lasers with the net anomalous dispersion. Three types of relative motions of solitons are found by solving the coupled complex NLSEs. When the pumping strength E_s is lower (e.g., E_s=70 pJ), two solitons always have exactly the same physics properties throughout their evolution and their separation approaches a fixed value (e.g., 1.9 ns). In this case, two solitons behave as a unit and are regarded as a static soliton pair. Contrarily, one of two solitons or both oscillate with approximately fixed amplitude of relative motions and a periodic round-trip number by appropriately enhancing E_s (e.g., E_s=81 or 85 pJ). Two solitons periodically attract and repel each other with respect to the round-trip number N. In this case, two solitons are regarded as a dynamic soliton pair. The P2P separation of static and dynamic soliton pairs is over two orders of magnitude larger than the pulse duration (Figs. 2 to 4).

The numerical simulations show that the relative motion of solitons attributes to the phase shift, which corresponds to the instantaneous frequency at pulse peak to be nonzero. When two solitons collide, they never pass through each other and the transfers of energy and information of solitons are transited by a virtual soliton. After the collision between two solitons, their shapes do not change, but their phases shift and relative motions change. The theoretical results demonstrate that the separation of neighboring solitons in laser cavity is about several hundreds of ps to several ns. The theoretical predictions are in good agreement with the experimental results. Our theoretical results

successfully interpret why the intracavity solitons have erratic relative motions and stabilize themselves at more or less random relative positions. In addition, the particle-like behavior of solitons can help us to better understand real particles.

ACKNOWLEDGMENTS

This work was supported by the National Natural Science Foundation of China under Grants No. 10874239 and No. 10604066. The author would especially like to thank Xiaohui Li, Dong Mao and Lina Duan for help with the experiments.

[1] H. Zhang, Q. Bao, D. Tang, L. Zhao, and K. Loh, Appl. Phys. Lett. **95**, 141103 (2009); D. Mao, X.M. Liu, L.R. Wang, X.H. Hu, and H. Lu, Laser Phys. Lett. **8**, 134 (2011).

[2] M. Stratmann, T. Pagel, and F. Mitschke, Phys. Rev. Lett., **95**, 143902 (2005).

[3] X. M. Liu, Phys. Rev. A **81**, 023811 (2010); X.M. Liu, L.R. Wang, X.H. Li, H.B. Sun, A.X. Lin, K.Q. Lu, Y.S. Wang, and W. Zhao, Opt. Express **17**, 8506 (2009).

[4] Z.P. Sun, D. Popa, T. Hasan, F. Torrisi, F. Wang, E. J. R. Kelleher, J. C. Travers, V. Nicolosi, and A. C. Ferrari, Nano Res. **3**, 653 (2010).

[5] S. Chouli and P. Grelu, Phys. Rev. A **81**, 063829 (2010).

[6] K. Tamura, H. A. Haus, and E. P. Ippen, Electron. Lett. **28**, 2226 (1992).

[7] X. M. Liu, Phys. Rev. A **82**, 063834 (2010).

[8] D. Y. Tang, L. M. Zhao, B. Zhao, and A. Q. Liu, Phys. Rev. A **72**, 043816 (2005).

[9] A. Komarov, H. Leblond, and F. Sanchez, Phys. Rev. E **72**, 025604 (2005).

[10] A. Komarov, H. Leblond, and F. Sanchez, Phys. Rev. A **71**, 053809 (2005).

[11] F. Amrani, M. Salhi, P. Grelu, H. Leblond, and F. Sanchez, Opt. Lett. **36**, 1545 (2011).

[12] X. M. Liu, Phys. Rev. A **84**, 023835 (2011)

[13] E.D. Farnum, B.G. Bale, J.N. Kutz, Phys. Rev. A **81**, 033851 (2010).

[14] R. Weill, B. Vodonos, A. Gordon, O. Gat, and B. Fischer, Phys. Rev. E **76**, 031112 (2007).

[15] X.M. Liu, Phys. Rev. A **81**, 053819 (2010); **82**, 053808 (2010).

[16] X.M. Liu, Opt. Express **19**, 5874 (2011).

[17] G. Agrawal, IEEE Photon. Technolo. Lett. **2**, 875 (1990).

[18] G. P. Agrawal, *Nonlinear Fiber Optics*, 4th edition (Academic Press, Boston, 2007).

[19] N. Benes, A. Kasman, and K. Young, J. Nonlinear Sci. **16**, 179 (2006)

[20] L. Motta, entry on "Feynman Diagrams," *Science World*: http://scienceworld.wolfram.com/physics/FeynmanDiagram.html

[21] http://kasmana.people.cofc.edu/SOLITONPICS/